

STM-induced desorption of hydrogen from Co nanoislands

M. Sicot, O. Kurnosikov, O. A. O. Adam, H. J. M. Swagten, and B. Koopmans

*Department of Applied Physics, Center for Nanomaterials and COBRA Research Institute, Eindhoven University of Technology,
P.O. Box 513, 5600 MB Eindhoven, The Netherlands*

(Received 9 July 2007; revised manuscript received 26 September 2007; published 16 January 2008)

Using low-temperature scanning tunneling microscopy (STM) and spectroscopy, we have studied the effects of H₂ adsorption at 10 K on the electronic properties of nanometer-scale triangular Co islands deposited on Cu(111). Before H₂ adsorption, two reported surface states are observed. However, after adsorption, both are quenched. In addition, we found that total removal of the adsorbate from the surface of the islands can be induced by the STM tip. As the tip affects only selected islands without perturbing neighboring islands, this process can be used to individually control the electronic properties of the Co nanoparticles. In particular, total desorption fully recovers the surface electronic features of the clean islands. Direct and indirect desorption mechanisms are discussed in relation to these experimental data.

DOI: [10.1103/PhysRevB.77.035417](https://doi.org/10.1103/PhysRevB.77.035417)

PACS number(s): 68.37.Ef, 68.43.Rs, 73.20.-r, 73.22.-f

I. INTRODUCTION

Nanometer-sized magnetic particles have attracted considerable attention due to their potential impact on high-density magnetic data storage. A promising system is composed of nanoparticles of controllable shape and size with perpendicular magnetic anisotropy (PMA) and high coercivity. An additional challenge is to tune these appealing magnetic properties particle by particle. In these systems, the size, the thickness, and the substrate are relevant parameters since they have a strong influence on the direction of the easy axis and the Curie temperature. When the magnetic domain structure depends strongly on surface anisotropy, it is also possible to use surface chemisorption to rotate the magnetic easy axis¹⁻³ or to obtain dead magnetic layers.⁴⁻⁷ These modifications are often reversible since thermal annealing allows for total desorption of the adsorbate. However, it is important to realize that desorption occurs for all particles affecting the entire system. In this paper, we present an alternative way to tune individually the electronic properties of nanoparticles by controlled adsorption and desorption induced by tunneling electrons from a scanning tunneling microscope (STM) tip. Indeed, it was shown that STM is not only able to probe at a (sub)nanometer scale but also can be used to manipulate atoms^{8,9} or build small devices.¹⁰ In our case, we took advantage of the fact that a STM tip can supply high current densities and thus induce desorption of atoms or molecules at the nanometer scale to uniquely modify the properties of individual nanoparticles. Moreover, as nanoparticles show unusual properties as compared to bulk, adsorption of a chemical species on a geometrical confined area may eventually lead to new properties.¹¹⁻¹⁵ Contrary to bulk metals and thin films, only a few studies have been devoted to the adsorption on magnetic nanoparticles.¹⁶⁻¹⁹ Therefore, it is of fundamental interest to study adsorption on magnetic nanoparticles and its effect on their electronic properties.

We study the Co/Cu(111) system since it is very attractive in terms of growth mode, perpendicular magnetic anisotropy, and high coercivity, and moreover, it has been extensively studied for its interesting magnetic surface properties.²⁰⁻²⁴ In the submonolayer coverage regime, trian-

gular and flat nanoislands of 10–30 nm size and two layer height exhibit PMA with a high coercivity of 1.0–1.5 T at $T=13$ K as shown by spin-polarized STM.²⁵ In the present paper, we focus on the influence of gaseous H₂ adsorption on the electronic properties of Co nanoislands at 10 K and on hydrogen desorption induced by STM at 5 K. Hydrogen is used as adsorbate since desorption of atomic hydrogen from semiconductor surfaces by STM has been extensively studied and desorption mechanisms have been identified and well characterized.²⁷ We extend this effect to ferromagnetic nanoparticles. Moreover, it has been reported that this adsorbate may change the magnetization of the surface layer through the hybridization of the $1s$ level with $3d$ electrons responsible for the magnetism.²⁸⁻³⁰ An additional advantage is that hydrogen has been used extensively for its simplicity and allows for theoretical calculations.³¹ Finally, dihydrogen is the most predominant residual gas in a stainless steel vacuum environment. It can desorb from walls and condense on a cold sample surface producing a contamination layer. As the key electronic feature of these Co islands is a minority d -like orbital resonant surface state,^{32,33} and given the fact that surface states are very sensitive to adsorption, the presence of such adsorbate can therefore lead to erroneous interpretation when studying magnetic properties by spin-polarized STM.

In our study, the differential conductance mapping mode is used to directly visualize the electronic state of the particles at the nanometer scale. We show that the d -like surface state is shifted downward in energy after hydrogen adsorption. Moreover, we show the ability to uniquely tune the electronic properties of each individual nanoisland by adsorption and controlled H desorption using the tunneling current from a scanning tunneling tip. We explain the H desorption from a Co surface in terms of interaction with tunneling electrons. This work clearly demonstrates the possibility to manipulate the surface electronic features of magnetic nano-objects by interface engineering.

II. EXPERIMENT

The experiments were performed in an ultrahigh vacuum (UHV) system composed of three connected chambers: a

preparation chamber for tip and sample cleaning treatments, a deposition chamber equipped with surface characterization tools, and a chamber with an “Omicron” low-temperature STM. The base pressure in the deposition and STM chambers is in the low 10^{-11} Torr range. The Cu(111) single crystal was cleaned by repeated cycles of Ar^+ sputtering and annealing to 850 K. Cobalt was evaporated with an electron beam evaporator at a rate of 0.1 monolayer/min. During Co deposition at room temperature, the pressure in the chamber is about 5.0×10^{-11} Torr. After deposition, the sample is transferred as fast as possible (~ 5 min) to the STM chamber where the temperature is already kept at $T=5$ K. Thus, the sample is directly cooled down to 5 K in order to avoid intermixing between Co and Cu, which occurs at higher temperatures. We used polycrystalline W tips which were electrochemically etched *ex situ* and cleaned under UHV conditions by electron bombardment. All microscopy and spectroscopy measurements were performed at $T=5$ K. For spectroscopy, the tip was initially stabilized at a sample bias voltage $U_s = -0.2$ V and a tunneling current $I_s = 2.0$ nA. The feedback loop was then open and the bias voltage was swept from -1.0 to 1.0 V. The differential conductance (dI/dU) was measured by the lock-in technique. For Co, spectral curves were measured inside a small area located in the center of the island since it was shown that the electronic properties are strongly modified in the rim area.²⁶ For adsorption experiments, samples were exposed to molecular hydrogen by means of a high precision leak valve. During H_2 exposure, the sample was located in the STM chamber with a substrate temperature of about 10 K. This slight temperature increase compared to 5 K is due to the opening of the radiation shields during this procedure.

III. RESULTS AND DISCUSSION

A. Clean Co on Cu(111)

First, we consider Co nanoislands before H_2 adsorption. In the submonolayer coverage regime, triangular Co islands with a bilayer height are observed. Their base length is typically 10–30 nm. Smaller islands (3–4 nm) have a more rounded shape. Two orientations are observed corresponding to two different stacking sequences: fcc and hcp or fcc faulted.^{25,33,34} The electronic properties of these islands are further investigated by scanning tunneling spectroscopy (STS). We compare islands of similar size and orientations since it was shown that electronic properties are slightly different between fcc and hcp oriented islands.^{25,33} In addition, the size might also modify the energy of the surface state due to different strains. Islands exhibit two surface states in agreement with previous works.^{25,33} In Fig. 1(a), the (dI/dU) spectrum shows a very sharp peak at -0.3 V. This peak is attributed to a minority d -like resonant surface state.^{25,32,33} We also observe a free electron surface state that is not visible on the (dI/dU) spectrum but can be visualized by recording a (dI/dU) map at bias voltages greater than -0.15 V.^{25,33} Indeed, the differential conductance map [Fig. 1(b)] shows quantum interference patterns due to the finite lateral size^{35–37} of the Co double layer and scattering of sp

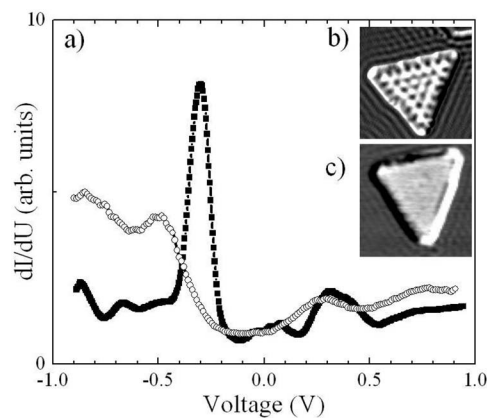


FIG. 1. (a) (dI/dU) spectra at 5 K on a Co nanoisland before (squares) and after (open circles) H_2 exposure of 42 L. The insets show the $18 \times 18 \text{ nm}^2$ (dI/dU) maps obtained at $U = +0.4$ V and $I = 2.0$ nA (b) before and (c) after adsorption of H_2 .

majority electrons.³³ We also checked the properties of the Cu substrate in between Co islands. The STS obtained on the Cu(111) substrate (not shown here) reveals the surface state at -0.4 V.^{38,39} As surface states are easily quenched by defects or impurities, their presence on both the substrate and the nanoislands is direct evidence of the cleanliness of our epitaxial system.

B. Hydrogen adsorption

Next, we study the modifications of the electronic properties of Co induced by adsorption of hydrogen at $T=10$ K. After hydrogen exposure of 1 L ($1 \text{ L} = 10^{-6}$ Torr s), no change is observed in the (dI/dU) spectrum in comparison with clean islands. After exposure of 16 L, a small part of the islands is affected by the adsorbate which may be explained by a variation of the sticking coefficient with the stacking and size of the islands. Upon exposure of 42 L, the (dI/dU) spectra of all islands differ strongly both in shape and in intensity in comparison with the clean islands. Figure 1(a) shows that instead of a pronounced peak at -0.3 V, a broad peak with a smaller intensity centered at -0.5 V is found. In addition, the quantum interferences due to the dispersive state are no more visible on (dI/dU) maps, as shown in Fig. 1(c). Thus, adsorption of hydrogen at low temperature leads to quenching of the two Co surface states. Himpsel and Eastman also observed that the peak corresponding to the resonant surface state for Co(0001) thin films completely vanishes⁴⁰ after adsorption of atomic hydrogen. Moreover, sp -like and d -like surface states of Ni(111) are quenched or shifted when H is adsorbed at $T=150$ K.⁴¹

To find out how the d -like surface state is spatially affected by hydrogen adsorption, we made (dI/dU) maps at its peak position of -0.3 V. As the presence of hydrogen quenches this d localized surface state, an area of low conductance can be interpreted as an adsorption area. Figure 2(a) shows a conductance map obtained on clean islands. They all exhibit a high conductance at -0.3 V across their entire surface implying that the surface state is present on the whole

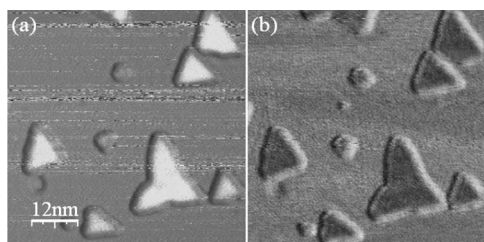


FIG. 2. (dI/dU) maps obtained at $U=-0.3$ V and $I=2.0$ nA at 5 K (a) before and (b) after H_2 exposure of 42 L. Bright colors correspond to a high conductance.

surface of individual islands. The conductance map measured on the same area after hydrogen adsorption of 42 L is shown in Fig. 2(b). A homogeneous but low conductance is observed. This homogeneity can be explained either by a saturated surface or by the delocalization of the adsorbate on the surface of the entire island.

C. Hydrogen desorption

Beyond the fact that hydrogen strongly modifies the Co electronic properties, we now show the ability to use the STM tip to remove it from the Co surface. Surprisingly, the electronic properties of hydrogen-terminated Co islands can be changed by the tunneling current coming from the tip. We experimentally observed that changes occur when sweeping the bias voltage from -1.0 to 1.0 V in the spectroscopic mode. By repeating this voltage ramp on the same island in the same area, strong modifications of the Co electronic properties are induced and observed in the (dI/dU) spectra. Figure 3 shows successive normalized spectra recorded one after another with a time between two spectra of about 1 min. Here, the ratio of differential to total conductance provides a relatively direct measure of the surface density of states of the sample. The curve labeled “1” corresponds to the first measurement taken in the center of one particular island. As described in Fig. 1(a), the main spectroscopic fea-

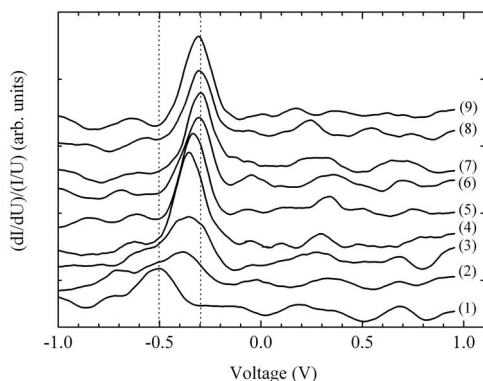


FIG. 3. Normalized conductance at 5 K on a Co nanoisland firstly exposed to hydrogen at 10 K. The spectrum labeled 1 is the first measurement performed in the center the Co nanoisland. Spectra labeled 7, 8, and 9 correspond to the stable and irreversible state. Spectra 1 to 9 are the successive measurements. All curves are vertically shifted for clarity.

ture is a broad peak centered at -0.5 V. When repeating the voltage ramp, a gradual shift in energy accompanied by an increase in intensity is observed for this main peak. After several repetitions, successive spectra labeled as “7,” “8,” and “9” in Fig. 3 all show the same spectroscopic feature at -0.3 V which is stable and irreversible in time. This state is the same as observed for samples before adsorption in Fig. 1(a) whose main feature is the d resonant state at -0.3 V. It is noteworthy that the sequence shown in Fig. 3 has been reproduced about 200 times on different islands and with different tips. However, the number of repetitions necessary to obtain the final state depends on the size of the islands. We define the energy shift as $\Delta E=E-E_0$, where E is the energy of the main peak below the Fermi level and E_0 is the energy of the d surface state of the clean islands. With that definition, the maximum ΔE observed value is equal to -0.2 eV whereas the minimum value is zero and corresponds to a clean surface.

We can conclude that the presence of the adsorbate on the Co surface leads to a strong energy shift of the initial d -like surface state down to -0.5 eV due to interaction between Co and the adsorbate that modifies the surface potential. The energy shift might be related to the amount of adsorbate on the surface. When sweeping the bias voltage from -1.0 to 1.0 V with the feedback loop open, the tunneling current strongly varies. In our experiments, this variation can be as high as 30 nA depending on the tunnel junction which is formed by the tip and the Co island. Exposing the island surface to such a high tunneling current induces desorption of a certain amount of the adsorbate. In fact, tunneling electrons can interact with adsorbed molecules or atoms and then give enough energy to overcome the desorption barrier. The desorption mechanisms involved will be discussed later. As the energy shift might be related to the amount of adsorbate on the surface, the following spectra will show a slight energy shift toward higher energies. The final energetic position of -0.3 eV is reached when hydrogen is totally desorbed. It must be emphasized that states at -0.5 and -0.3 eV are actually one and unique state but shifted in energy. Indeed, in the case of two different states, we expect to see two spectral peaks of different relative intensities which depend on the amount of H adsorbed. Therefore, the exact character of our experimentally observed intermediate state is not clear yet and might strongly depend on the hybridization with hydrogen. Note that this cleaning effect is no longer observable when reducing the range of the bias voltage from ± 1.0 to ± 0.4 V. In that limited range, the Co electronic properties are no longer affected even after many repetitions, and we can utilize this voltage range to check the presence of hydrogen without perturbing the system. This evidence of a threshold in energy will be discussed later in this paper. As a provisional conclusion, the tunneling tip acts not only as a probe but also induces electronic changes at the surface of Co nanoislands exposed to an adsorbate and thus can be used to clean contaminated islands.

In order to investigate how far the cleaning effect spread from the tip position, (dI/dU) maps were recorded at -0.3 V. As we have seen before, at this bias voltage, we can discriminate between the hydrogen-terminated surface and clean Co surface since the conductance at -0.3 V is low

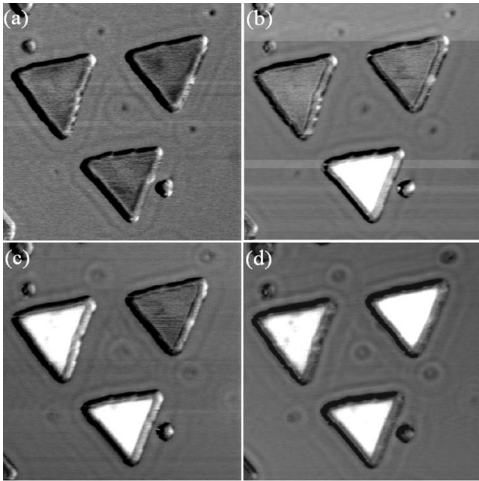


FIG. 4. Illustration of the selective desorption process induced by tunneling current. $46 \times 46 \text{ nm}^2$ (dI/dU) maps obtained at $U = -0.3 \text{ V}$ and $I = 2.0 \text{ nA}$ at 5 K after adsorption of hydrogen at 10 K (a) before the cleaning procedure. The cleaning procedure was applied to (b) the bottom island, (c) the top left island, and (d) the top right island. Bright colors correspond to a high differential conductance.

when hydrogen is adsorbed and is high for the clean Co surface. Figure 4 illustrates a sequence of selective hydrogen desorption from three similar islands. First, in Fig. 4(a), the (dI/dU) map was recorded on islands just after H adsorption. All islands exhibit the same low differential conductance reflecting their identical electronic properties similar to those observed in Fig. 3(b). Second, the tip was positioned right at the center of the bottom island. Then, the bias voltage was ramped from -1.0 to $+1.0 \text{ V}$. During that ramp, the feedback loop was open allowing the tunneling current to vary. Scanning of the bias voltage was performed until the surface state appeared at -0.3 V . Third, the conductance map after this action is recorded and gives Fig. 4(b). The conductance of the altered bottom island is now high and homogeneous across the whole surface. In contrast, all surrounding islands show the same low conductance, as observed in Fig. 4(a); their electronic properties are unaffected by the action of the tip on the bottom island. Consequently, although the tip is located on one point during the STS experiment, the whole surface is cleaned. Desorption is thus a nonlocal process since it occurs on the entire surface of the island but seems to be geometrically restricted by the islands' edges. To prove the reproducibility of this procedure, we repeat the experiment on the top left island [Fig. 4(c)] and on the top right island [Fig. 4(d)].⁴² The comparison between Figs. 4(a) and 4(d) illustrates the efficiency of this process in modifying the electronic properties of the nanoislands. Finally, after the cleaning procedure was performed on these three islands, (dI/dU) maps at positive bias voltages show quantum interferences as discussed earlier [Fig. 1(b)]. Therefore, desorption induced by the tunneling electrons allows us to recover original electronic properties of clean islands, which includes the localized d and the dispersive surface states. This sequence thus illustrates electron stimulated desorption at low

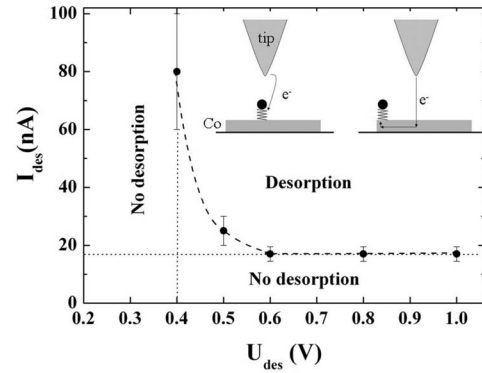


FIG. 5. Occurrence of desorption as a function of the tunneling current I and the bias voltage U . For each (I, U) couple situated below the curve, no desorption is induced on Co islands' surface. On the contrary, above this area, desorption is observed. The dashed line is a guide for the eyes. The inset is a schematic diagram showing two possible paths for the electrons before interaction with the adsorbate.

energy on the surface of ferromagnetic nanoparticles.

D. Desorption mechanisms

In order to investigate the dependence of desorption on tunneling current and bias voltage, we keep the bias voltage constant while controlling the tunneling current. More specifically, in that part, the tunneling current is ramped at constant bias voltage with closed feedback loop. The tip is positioned above an island previously covered with hydrogen, and the set point of the tunneling current was gradually increased from 2.0 nA to a chosen current value I_0 . In response of current changes during that ramp, the feedback moves the tip a little closer toward the sample. However, the actual displacement of the tip is of the order of 1 \AA regarding the exponential dependency of the tunneling current on the tip-sample distance. We assume that this displacement itself has no influence on the hydrogen. The duration of the current ramp procedure is the same as the previous (dI/dU) spectroscopy in the range of $\pm 1.0 \text{ V}$, that is, from one to a few seconds. Subsequently, in order to estimate the result of this current ramp on the electronic state of the Co nanoislands, STS is performed on the limited range between -0.4 and $+0.4 \text{ V}$. As mentioned above, this limited range does not lead to desorption. When it is observed that $\Delta E \leq -0.2 \text{ V}$ corresponding to the absence or onset of desorption, we move to another island and then increase I_0 , and repeat the procedure. Once I_0 is high enough to lead to total desorption for which ΔE is equal to zero, we have established the desorption parameters I_{des} at a voltage U_{des} (see Fig. 5). Doing this with different values of bias voltage, current and voltage thresholds can be systematically determined. We use this procedure with positive bias voltage.

Figure 5 reveals two regions. The first one is situated under the curve and corresponds to the regime without any hydrogen desorption. The second one is situated above the curve and corresponds to complete desorption. The uncertainty in the data points corresponds to the intermediate case

when the (dI/dU) curve indicates an incomplete desorption: the characteristic peak in the (dI/dU) spectrum is shifted only a little. Remarkably, the diagram shows the presence of two thresholds: a current threshold of about 15–20 nA and a voltage threshold of about 0.4–0.5 V. This voltage threshold was already partially observed in previous experiments in the spectroscopic mode. Indeed, whereas sweeping the bias voltage from -1.0 to $+1.0$ V leads to partial desorption, using a bias voltage between -0.4 and $+0.4$ V does not modify the islands' properties even after many repetitions. The bias voltage threshold is not fully abrupt: in the 0.4–0.5 V range, the current required for desorption varies gradually when approaching the value of 0.4 V. For a voltage larger than 0.5 V, the system can be characterized with a uniform current threshold of approximately 18 nA.

Considering this dependency and the thresholds, the physical mechanisms involved in hydrogen desorption from the Co surface can be identified. In the following, we discuss these mechanisms in detail. First of all, the question to answer is what is the nature of the adsorbate, dissociative atomic or molecular? Indeed, energies that reflect the interaction with the substrate for atomic or molecular hydrogen are of different orders of magnitude. For atomic adsorbates, the binding energies are several eV, whereas for physisorbed H_2 molecules, typical energies are in the 40–150 meV range depending on the system.^{43–45} Due to these low values for H_2 , it is quite impossible to observe molecules at temperatures higher than 20 K. When a H_2 molecule interacts with a metallic surface, it has to overcome one or more activation barriers to reach the chemisorbed state. As it was shown that the dissociation process is mainly governed by the density of d electrons at the Fermi level of the substrate,⁴⁶ transition and noble metals do not react similarly toward molecular hydrogen adsorption. Transition metals allow an easy dissociative process due to their low or inexistent activation barrier. On the contrary, for noble metals such as Au(111), Cu(111) and Ag(111), large activation barriers exist and do not provide easy dissociation. For example, it was shown that H_2 molecules physisorb on flat noble metals at 5 K (Refs. 44 and 45) and, in particular, on Cu(111).⁴⁷ As a first conclusion, we assume that after the inlet of hydrogen, atomic H is present on the surface of our Co nanoislands whereas physisorption occurs on the copper substrate. In our case, a strong argument in favor of dissociative adsorption on the Co surface relies on the observation of the cleaning process occurring at 77 K as well.

Let us now consider desorption mechanisms. From studies of STM-induced desorption,^{48–52} two distinct mechanisms have been identified: (i) desorption via vibrational excitation^{53–56} and (ii) desorption by electron excitation.^{44,45} In the first vibrational mechanism, high current densities supplied by the STM induce multiple-vibrational excitations through inelastic electron tunneling.⁵³ The gain of vibrational energy by the harmonic oscillator formed by the substrate-adsorbate atoms or by intramolecular atoms of the adsorbed molecules can finally overcome the potential barrier and lead to desorption. The second mechanism of electron excitation occurs for higher energies and with a higher yield. In that case, a single electron transition from a substrate-adsorbate atom bonding to an antibonding state leads to desorption.

Therefore, a minimal energy corresponding to the transition is necessary and results in a threshold of bias voltage in a STM experiment. For atomic H on Co, the desorption via direct electron excitation should occur for an energy greater than 2.6 eV according to theoretical calculations of the binding energy of H on a Co substrate.³¹ Since in our experiment we observed that the energy corresponding to the onset of desorption is much lower than the typical binding energy of a single atomic hydrogen bond with a metallic substrate, we can rule out a direct electron desorption by electron excitation in our range of bias voltage. As a result of these considerations, we propose that the vibrational excitation mechanism is capable of explaining our experimental observations. As the energy of 0.4 eV is higher than the typical vibrational energies of the transition metal-H mode,⁵⁷ we could relate this energy to a more complex mode involving more than one H atom. As shown in Fig. 4, the desorption occurs on the entire surface of the island while injection of electrons is pointlike. We point out two possible explanations for this nonlocal indirect desorption process. First, electrons can initiate hydrogen motion by lateral hopping^{58–60} and increase hydrogen mobility on the surface. Second, in the case of indirect excitations by hot electrons in the metal, electrons are the mobile particles which carry the energy and can transport it through the whole surface, as reported recently,⁶¹ whereas hydrogen atoms remain fixed, as illustrated in the inset of Fig. 5. Nevertheless, we do not exclude that other mechanisms could be consistent with our data, which is a subject for future work in this field.

The analysis of the current threshold gives additional insight into the desorption mechanism. The presence of such a threshold indicates that desorption is a multiple electron process. In the case of a one-particle process, as soon as the electron has enough energy, it can induce H desorption. Consequently, a long surface exposure to a tunnel current at a bias voltage higher than the voltage threshold of 0.4 V is expected to induce desorption whatever the current value and even at a current below the threshold. Experimentally, this is clearly not the case since we found that a long injection of current below the current threshold shows no cleaning process. From the current threshold value of 18 nA and assuming a two particle process, we can estimate a characteristic time of 10 ps. This time could be considered either as a relaxation time between two vibrational levels due to energy transfer to metal phonons or a dwell time of hydrogen on one atomic site.

IV. CONCLUSION AND OUTLOOK

In summary, we studied hydrogen adsorption on Co nanoislands grown epitaxially on Cu(111) by scanning tunneling microscopy and/or spectroscopy at $T=5$ K. We found that the presence of the adsorbate strongly affects the two well-known Co surface states. The Co Shockley state is quenched, whereas the minority d surface state is shifted to lower energies down to -0.5 eV. Most importantly, we show that hydrogen could be totally removed from the Co surface by desorption induced by tunneling electrons.

By analyzing the spatial variation of differential conductance, we show that desorption occurs on a surface of a few

nanometer squares and is limited to a single individual island. We have determined relevant parameters for desorption. Hydrogen desorbs from the Co surface when the tunneling current is larger than 18 nA and electrons have an energy greater than 0.5 eV. This relatively low energy suggests that the desorption proceeds via a vibrational excitation mechanism. Nonlocal desorption is explained in terms of interaction of H atoms with electrons leading to H motion or of hot-electron transport on the Co surface. We expect that further theoretical modeling could help us to relate the bias voltage threshold value to the energy of a vibrational mode involving Co and H atoms.

Hydrogen desorption from a surface of flat ferromagnetic nanoparticles by tunneling electrons has been demonstrated. We took advantage of this local desorption to uniquely tune

the electronic properties of each individual nanoisland using the tunneling current from the STM tip. This study could be extended to similar systems involving ferromagnetic nanoislands. Different materials would modify the value of the voltage threshold since it is related to the interaction between the material and the adsorbate. We might use desorption to selectively create preferential surfaces of a few nanometer squares for further adsorption of atoms or molecules.

ACKNOWLEDGMENTS

This work was supported by the Dutch Technology Foundation (STW) via the NWO VICI-grant “spintronics,” as well as the Dutch Foundation for the Fundamental Research of Matter (FOM).

-
- ¹Daiju Matsumura, Toshihiko Yokoyama, Kenta Amemiya, Soichiro Kitagawa, and Toshiaki Ohta, *Phys. Rev. B* **66**, 024402 (2002).
- ²S. Hope, E. Gu, B. Choi, and J. A. C. Bland, *Phys. Rev. Lett.* **80**, 1750 (1998).
- ³H. J. Elmers, J. Hauschild, and U. Gradmann, *J. Magn. Magn. Mater.* **198-199**, 222 (1999).
- ⁴M. Weinert and J. W. Davenport, *Phys. Rev. Lett.* **54**, 1547 (1985).
- ⁵C. S. Feigerle, A. Seiler, J. L. Peña, R. J. Celotta, and D. T. Pierce, *Phys. Rev. Lett.* **56**, 2207 (1986).
- ⁶B. Sinković, P. D. Johnson, N. B. Brookes, A. Clarke, and N. V. Smith, *Phys. Rev. B* **52**, R6955 (1995).
- ⁷S. R. Chubb and W. E. Pickett, *Phys. Rev. B* **38**, 10227 (1988).
- ⁸D. M. Eigler and E. K. Schweizer, *Nature (London)* **344**, 524 (1990).
- ⁹L. Bartels, G. Meyer, and K.-H. Rieder, *Phys. Rev. Lett.* **79**, 697 (1997).
- ¹⁰Laetitia Soukiassian, Andrew J. Mayne, Marilena Carbone, and Gérald Dujardin, *Surf. Sci.* **528**, 121 (2003).
- ¹¹K. D. Rendulic, A. Winkler, and H. P. Steinrück, *Surf. Sci.* **185**, 469 (1987).
- ¹²A.-S. Mårtensson, C. Nyberg, and S. Andersson, *Surf. Sci.* **205**, 12 (1988).
- ¹³Peter Schilbe, Susanne Siebentritt, Roland Pues, and Karl-Heinz Rieder, *Surf. Sci.* **360**, 157 (1996).
- ¹⁴L. Barrio, P. Liu, J. A. Rodríguez, J. M. Campos-Martín, and J. L. G. Fierro, *J. Chem. Phys.* **125**, 164715 (2006).
- ¹⁵K. Svensson, L. Bengtsson, J. Bellman, M. Hassel, M. Persson, and S. Andersson, *Phys. Rev. Lett.* **83**, 124 (1999).
- ¹⁶J. Wiebe, L. Sacharow, A. Wachowiak, G. Bihlmayer, S. Heinze, S. Blügel, M. Morgenstern, and R. Wiesendanger, *Phys. Rev. B* **70**, 035404 (2004).
- ¹⁷L. Berbil-Bautista, S. Krause, T. Hänke, M. Bode, and R. Wiesendanger, *Surf. Sci.* **600**, L20 (2006).
- ¹⁸H. J. Elmers, J. Hauschild, and U. Gradmann, *Phys. Rev. B* **59**, 3688 (1999).
- ¹⁹K. von Bergmann, M. Bode, A. Kubetzka, M. Heide, S. Blügel, and R. Wiesendanger, *Phys. Rev. Lett.* **92**, 046801 (2004).
- ²⁰U. Alkemper, C. Carbone, E. Vescovo, W. Eberhardt, O. Rader, and W. Gudat, *Phys. Rev. B* **50**, 17496 (1994).
- ²¹F. Huang, M. T. Kief, G. J. Mankey, and R. F. Willis, *Phys. Rev. B* **49**, 3962 (1994).
- ²²F. Schreiber, A. Soliman, P. Bödeker, R. Meckenstock, K. Bröhl, J. Pelzl, and I. A. Garifullin, *J. Appl. Phys.* **75**, 6492 (1994).
- ²³J. Izquierdo, A. Vega, and L. C. Balbás, *Phys. Rev. B* **55**, 445 (1997).
- ²⁴J. Camarero, J. J. de Miguel, R. Miranda, V. Raposo, and A. Hernando, *Phys. Rev. B* **64**, 125406 (2001).
- ²⁵O. Pietzsch, A. Kubetzka, M. Bode, and R. Wiesendanger, *Phys. Rev. Lett.* **92**, 057202 (2004).
- ²⁶O. Pietzsch, S. Okatov, A. Kubetzka, M. Bode, S. Heinze, A. Lichtenstein, and R. Wiesendanger, *Phys. Rev. Lett.* **96**, 237203 (2006).
- ²⁷See, for example, A. J. Mayne, D. Riedel, G. Comtet, and G. Dujardin, *Prog. Surf. Sci.* **81**, 1 (2006), and references therein.
- ²⁸Carlos R. Abeledo and P. W. Selwood, *J. Chem. Phys.* **37**, 2709 (1962).
- ²⁹R. E. Dietz and P. W. Selwood, *J. Chem. Phys.* **35**, 270 (1961).
- ³⁰G. J. Mankey, M. T. Kief, F. Huang, and R. F. Willis, *J. Vac. Sci. Technol. A* **11**, 2034 (1993).
- ³¹D. J. Klink II and L. J. Broadbelt, *Surf. Sci.* **429**, 169 (1999).
- ³²M. A. Barral, M. Weissman, and A. M. Llois, *Phys. Rev. B* **72**, 125433 (2005).
- ³³L. Diekhöner, M. A. Schneider, A. N. Baranov, V. S. Stepanyuk, P. Bruno, and K. Kern, *Phys. Rev. Lett.* **90**, 236801 (2003).
- ³⁴A. L. Vázquez de Parga, F. J. García-Vidal, and R. Miranda, *Phys. Rev. Lett.* **85**, 4365 (2000).
- ³⁵O. Jeandupeux, L. Bürgi, A. Hirstein, H. Brune, and K. Kern, *Phys. Rev. B* **59**, 15926 (1999).
- ³⁶J. Li, W.-D. Schneider, S. Crampin, and R. Berndt, *Surf. Sci.* **422**, 95 (1999).
- ³⁷Stéphane Pons, Pierre Mallet, and Jean-Yves Veuillen, *Phys. Rev. B* **64**, 193408 (2001).
- ³⁸P. Heimann, H. Neddermeyer, and H. F. Roloff, *J. Phys. C* **10**, L17 (1977).
- ³⁹M. F. Crommie, C. P. Lutz, and D. M. Eigler, *Nature (London)* **363**, 524 (1993).
- ⁴⁰F. J. Himpsel and D. E. Eastman, *Phys. Rev. B* **20**, 3217 (1979).
- ⁴¹W. Eberhardt, F. Greuter, and E. W. Plummer, *Phys. Rev. Lett.*

- 46**, 1085 (1981).
- ⁴²The black dots observed on the top left islands are Cu adatoms as deduced from the topographic profile.
- ⁴³J. L. Seguin and J. Suzanne, *Surf. Sci.* **118**, L241 (1982).
- ⁴⁴S. Andersson and J. Harris, *Phys. Rev. Lett.* **48**, 545 (1982).
- ⁴⁵Ph. Avouris, D. Schmeisser, and J. E. Demuth, *Phys. Rev. Lett.* **48**, 199 (1982).
- ⁴⁶J. Harris and S. Andersson, *Phys. Rev. Lett.* **55**, 1583 (1985).
- ⁴⁷G. D. Kubiak, G. O. Sitz, and R. N. Zare, *J. Chem. Phys.* **83**, 2538 (1985).
- ⁴⁸R. S. Becker, G. S. Higashi, Y. J. Chabal, and A. J. Becker, *Phys. Rev. Lett.* **65**, 1917 (1990).
- ⁴⁹In-Whan Lyo and Ph. Avouris, *J. Chem. Phys.* **93**, 4479 (1990).
- ⁵⁰E. T. Foley, A. F. Kam, J. W. Lyding, and Ph. Avouris, *Phys. Rev. Lett.* **80**, 1336 (1998).
- ⁵¹T.-C. Shen, C. Wang, G. C. Abeln, J. R. Tucker, J. W. Lyding, Ph. Avouris, and R. E. Walkup, *Science* **268**, 1590 (1995).
- ⁵²T.-C. Shen and P. Avouris, *Surf. Sci.* **390**, 35 (1997).
- ⁵³R. E. Walkup, D. M. News, and Ph. Avouris, *Phys. Rev. B* **48**, 1858 (1993).
- ⁵⁴B. C. Stipe, M. A. Rezaei, W. Ho, S. Gao, M. Persson, and B. I. Lundqvist, *Phys. Rev. Lett.* **78**, 4410 (1997).
- ⁵⁵B. N. J. Persson and Ph. Avouris, *Surf. Sci.* **390**, 45 (1997).
- ⁵⁶L. Bartels, M. Wolf, T. Klamroth, P. Saalfrank, A. Kühnle, G. Meyer, and K.-H. Rieder, *Chem. Phys. Lett.* **313**, 544 (1999).
- ⁵⁷K. Christmann, *Surf. Sci. Rep.* **9**, 1 (1988), and references therein.
- ⁵⁸H. Ueba and B. N. J. Persson, *Surf. Sci.* **566-568**, 1 (2004).
- ⁵⁹B. N. J. Persson and H. Ueba, *Surf. Sci.* **502-503**, 18 (2002).
- ⁶⁰T. Komeda, Y. Kim, and Maki Kawai, *Surf. Sci.* **502-503**, 12 (2002).
- ⁶¹Peter Maksymovych, Daniel B. Dougherty, X.-Y. Zhu, and John T. Yates, Jr., *Phys. Rev. Lett.* **99**, 016101 (2007).